Edyta KUDLEK[1], Daniele SILVESTRI[2], Stanisław WACŁAWEK[2*], Vinod V.T. PADIL[2]
Martin STUCHLÍK[2], Lukáš VOLESKÝ[2], Pavel KEJZLAR[2] and Miroslav ČERNÍK[2]

TiO$_2$ IMMOBILISED ON BIOPOLYMER NANOFIBERS FOR THE REMOVAL OF BISPHENOL A AND DICLOFENAC FROM WATER

TiO$_2$ IMMOBILIZOWANY NA BIOPOLIMEROWYCH NANOWŁÓKNACH W CELU USUWANIA BISFENOLU A I DIKLOFENAKU Z WODY

Abstract: Recently electrospinning has gained significant attention due to unique possibilities to produce novel natural nanofibers and fabrics with controllable pore structure. The present study focuses on the fabrication of electrospun fibres based on gum karaya (GK), a natural tree gum, with polyvinyl alcohol (PVA), and functionalization of the membrane with TiO$_2$ nanoparticles with further methane plasma treatment. The GK/PVA/TiO$_2$ membrane was analyzed with several techniques including: fourier-transform infrared spectroscopy (FTIR), thermogravimetric analysis (TGA), scanning electron microscopy with energy dispersive X-ray spectroscopy (SEM-EDX), and water contact angle, in order to characterize its morphological and physicochemical properties. The GK/PVA/TiO$_2$ membrane was further successfully used for the degradation (under UV irradiation) of bisphenol A and diclofenac from aqueous solution. It was also observed that the degradation kinetics of these compounds are faster in comparison to the UV treatment alone.

Keywords: biopolymer nanofibers, TiO$_2$ nanoparticles, bisphenol A, diclofenac

Introduction

During the last few years, electrospinning has shown to be simple, versatile, and cost-effective technology, which generates non-woven fibers with high surface area to volume ratio, porosity and tunable porosity. Because of these properties this process seems to be a promising candidate for various applications especially tissue engineering applications [1].

Furthermore, electrospinning often allows to immobilize on fibers materials that can enhance their properties [2]. Many studies focused on implementation of silver [2], gold [3], magnetite [4] and zero-valent iron (ZVI) [5] nanoparticles on electrospun membranes in order to improve their properties. Titanium dioxide (TiO$_2$) is a transition metal oxide, in nature there can be found four polymorphs of TiO$_2$ [6]. According to Han et al. [7], TiO$_2$ in the nanoscale range has much better photocatalytic properties.

[1] Faculty of Energy and Environmental Engineering, Silesian University of Technology, ul. S. Konarskiego 18, 44-100 Gliwice, Poland, phone +48 32 237 24 78
[2] Centre for Nanomaterials, Advanced Technologies and Innovation, Technical University of Liberec, Studentská 1402/2, 461 17 Liberec 1, Czech Republic, phone +420 485 353 006
* Corresponding author: stanislaw.waclawek@tul.cz

TiO$_2$ is also often used supported with metal/metal oxide particles, creating composite material e.g. TiO$_2$-CdS [8], Bi$_2$S$_3$-TiO$_2$ [9], TiO$_2$-WO$_3$ [10], TiO$_2$-Fe$_2$O$_3$ [11], TiO$_2$-SnO$_2$ [12], or TiO$_2$-MoO$_3$ [13].

Nanoscale TiO$_2$ is white, fine (~25 nm) powder/pigment that has use in many industries. It can be applied as a white pigment for paints, cosmetics and foodstuffs or an additive to functional construction materials for air and water purification, self-cleaning or antimicrobial protection [14], and its photocatalytic activity was shown in many studies [15]. In addition, there were also several research works focusing on supplementing of TiO$_2$ on the electrospun membrane [15], although their application were aimed mainly on their filtration properties than the photocatalytic ones [16].

Trace organic contaminants are routinely found in raw and processed municipal wastewater and wastewater-impacted natural water bodies at trace levels ranging from a couple of ng per dm^3 to a few microgram per dm^3. The widespread occurrence of them such as industrial chemicals, pharmaceuticals and personal care products in sewage-impacted water bodies has brought up substantial worries owed to their possible harmful consequences on human health and marine ecology [17]. Therefore, there is a necessity to develop efficient methods for their decontamination.

Over the last few years, the application of biopolymers for removal of a large spectrum of pollutants from water has been studied [18]. Polymers like chitosan [19], cyclodextrin [20], cellulosic biopolymer [21], alginic acid [22], and guar gum [23] have been extensively studied for this purpose. Biopolymers have also been studied for stabilization of nanoparticles [24] e.g. gum karaya stabilized nano zero-valent iron particles [25]. Another often-studied topic over recent decades are the advanced oxidation processes (AOPs) [26], these processes are often used for the removal of various contaminants from water [27]. Among them, the photocatalysis with TiO$_2$ is of considerable interest recently [28].

The removal of trace organic contaminants (TrOCs; e.g. bisphenol A and diclofenac) from water and wastewater is of considerable interest since certain TrOCs have been found to potentially affect human health after prolonged exposure [29]. Yang et al. [29], studied bisphenol A and diclofenac degradation with biological treatment. It was observed therein that 80-90% removal of bisphenol A and approximately 55% removal of diclofenac can be achieved with a fungal membrane bioreactor treatment.

In this study, TiO$_2$ functionalized electrospun GK/PVA (gum karaya/polyvinyl alcohol) membrane was fabricated and characterised with various techniques including FTIR, TGA, SEM-EDX and water contact angle. In addition, this membrane was later used for the removal of two trace organic compounds (bisphenol A and diclofenac) under UV radiation and the kinetics of their degradation were calculated.
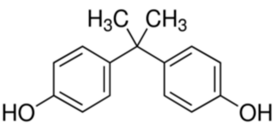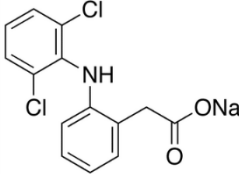
Materials and methods

Materials

All of the chemicals used in the experiments were analytical reagent grade. TiO$_2$ nanoparticle powder in the form of 99.7% anatase polyvinyl alcohol (PVA; Mw 88,000; degree of deacetylation 88%), and gum karaya were purchased from Sigma Aldrich. Micro pollutants i.e. diclofenac and bisphenol A were also purchased by Sigma Aldrich and their characteristics are presented in Table 1. Deionised water (18.2 MΩ·cm^{-1}) was prepared by an ELGA purelab flex system (ELGA, Veolia Water, Marlow, UK).

Table 1

Characteristics of compounds used in the experiments

Compound		
Name	Bisphenol A	Diclofenac sodium salt
Structural formula		
Characteristics		
Molecular formula	C$_{15}$H$_{16}$O$_2$	C$_{14}$H$_{10}$Cl$_2$NNaO$_2$
Molecular weight [g/mol]	228.29	318.13
Solubility in water [mg/dm^3]	300	50
pK_a	9.9	4.15
log K_{ow}	3.44	4.51

Electrospinning solutions and parameters

GK solution (deacetylated) (3 wt.%; with or without TiO$_2$ (1 wt.%) content) was prepared by dissolving it in deionised water. The PVA (10 wt.%) solution was prepared by heating at 90°C in a magnetic stirrer for 4 h. Then, the PVA solution was mixed with the GK solution in different ratios i.e. 0/100, 40/60, 50/50, 60/40, 70/30, 80/20, 90/10 and 100/0 (PVA/GK weight ratio) to determine a good spinability and uniform nanofiber size distribution. The electrospinning was carried out with a Nanospider electrospinning machine (NS IWS500U, Elmarco, Czech Republic) under the following conditions: spinning electrode width = 500 mm, effective nanofiber layer width = 200-500 mm; spinning distance = 130-280 mm, substrate speed = 0.015-1.95 m/min, process air flow = 20-150 m^3/h and voltage 0-50 kV.

Methane plasma treatment

The plasma treatment was done in a radio frequency plasma reactor (BalTec Maschinenbau AG, Pfäffikon, Switzerland). The plasma chamber was thoroughly purged with a continuous flow of the gas used during the treatment to reduce trace amounts of air and moisture. During the treatment, the gas flow was adjusted in order to keep a constant pressure of 0.2 mbar inside the chamber. A power of 20 W was applied. The duration of the treatment was varied from 2 min onwards. The plasma conditions were as follows: voltage 300 V; time 5 min; pressure 20 Pa and plasma gas purity 99.997%. The process parameters were as follows: electrode area 48 cm^2; inter-electrode distance 50 mm; chamber volume 1 dm^3.

Determination of water contact angle

Measurements of the water contact angle (ө) were used to determine the surface wettability of the membrane using the sessile drop method. The measurements were performed using OCA20 equipment (Data Physics, Germany) and SCA-20 software. The presented data are the average of three measurements.

ATR-FTIR

ATR-FTIR spectra were obtained with a resolution of 4 cm^{-1} at 4000-700 cm^{-1} using a germanium ATR crystal (NICOLET IZ10, Thermo Scientific, USA) equipped with a single reflection angle 45° horizontal ATR accessory.

Thermogravimetric analysis (TGA)

Thermal stability and composition of the PVA/GK, TiO$_2$ electrospun membrane, and plasma treated TiO$_2$ electrospun membrane were determined using TGA, Q500 (TA instruments, USA). The experimental atmosphere was nitrogen at a flow rate of 60 cm^3/min. The sample was heated from 30 to 700°C.

High pressure liquid chromatography (HPLC)

The concentration of organic micro pollutants in the solutions was determined on the basis of quantitative analysis with high performance liquid chromatography HPLC preceded with solid phase extraction SPE. BPA was extracted from the water samples by the use of Supelclean™ ENVI-18 tubes. The tube phase (C$_{18}$) was conditioned with 5 cm^3 of acetonitrile, 5 cm^3 methanol (both HPLC grade, ≥99.9%, Sigma-Aldrich) and next washed with distilled water of pH 7. Whereas for the extraction of DCF Supelclean™ ENVI-8 tube with a C$_8$ phase were used, which were conditioned only with 5 cm^3 methanol and also washed with pH 7 distilled water. After the extraction of water sample of a volume 20 cm^3 the column bed was dried for 5 min at vacuum. The analytes were eluted with 3 cm^3 of a mixture acetonitrile/methanol (60:40, v/v) for BPA and methanol (for DCF) and dried in a nitrogen stream. After dissolution of the samples in 100 cm^3 of methanol they were subjected to chromatographic analysis. HPLC by Varian (Warsaw, Poland) equipped with a UV-Vis detector (wavelength for BPA $\lambda = 218$ nm and for DCF $\lambda = 220$ nm) was used. Hypersil GOLD column by Thermo Scientific of length 25 cm, diameter 4.6 mm and granulation - 5 µm was used as the chromatographic column. The mobile phase consisted of a mixed water and methanol in the ratio of 85:15 (v/v).

Scanning electron microscope (SEM) and energy-dispersive X-ray spectroscopy (EDX) analysis

The composition and morphology of the electrospun TiO$_2$ membrane were studied using a scanning electron microscope with a beam current 12 to 40 nA and acceleration voltage 0.02 to 30 kV and with complete detection system with In-lens energy and angle selective backscatter detector (EsB), 4-quadrant solid-state backscattered detector (AsB) and Conventional secondary electron detector (Everhardt-Thornley) (ZEISS, Ultra/Plus, Germany). Ideally, specimens were permanently mounted onto stubs using slow-drying araldite or silver dag. The stub with the specimen was then sputter coated with a thin layer of gold to make the specimens conductive under high vacuum conditions. The processed specimen was subjected to SEM analysis. The EDX analysis was conducted to determine the presence of various elements in the electrospun TiO$_2$ membrane.

Adsorption tests

The water solutions were prepared on deionized water matrices with the addition of diclofenac and bisphenol A standards at a concentration of 0.5 mg/dm^3. The concentrations of pharmaceuticals were selected taking into account their solubility in water and maximal

environmental concentration in surface waters. The pH of the solutions was adjusted to 7 using 0.1 mol/dm³ HCl or 0.1 mol/dm³ NaOH.

UV treatment

Tests with UV and UV with immobilised TiO₂ on membrane (UV+TiO₂ membrane) in the water solution, were carried out in the laboratory batch reactor Heraeus (volume of 700 cm³). The reactor was equipped with a medium-pressure, immersed, mercury lamp of the power of 150 W placed in the cooling jacket made of the Duran 50 glass, which blocked radiation of wavelengths smaller than 300 nm. The reaction mixtures ware irradiated with wavelength ranged from UV to visible light. The process temperature was 20±1°C. The aeration of the reactor was based on an aeration pump of capacity 4 dm³ of air per min. This capacity was sufficient for the proper execution of a photocatalysis process. The radiation was carried out constantly for 60 minutes.

The optimal membrane dose (70 mg) was selected during the preliminary stage of the study. The contact time of the catalyst with treated water before its irradiation was established at 15 minutes. This step ensures the preadsorption of micro pollutants on the surface of the catalyst and membrane. It should be emphasized that the degree of adsorption determines the efficiency of the photochemical decomposition of the compound.

The kinetics interpretation of UV and UV/membrane processes was obtained using Langmuir-Hinshelwood [30] equation as a conjugated function of micro pollutant concentration and time:

$$r = \frac{\mathrm{d}C}{\mathrm{d}t} = k \cdot \left(\frac{KC}{1+KC} \right) \tag{1}$$

where: r - rate of reaction [mg/(dm³·min)]; C - concentration of organic compounds at any time t during degradation [mg/dm³]; k - reaction rate constant [1/min]; K - organic compounds adsorption equilibrium constant.

The oxidation of compounds during catalyzed UV processes assumes the form of pseudo-first order reaction, this allows for the calculation of the reaction rate constant according to equation:

$$-\ln\left(\frac{Ct}{C_0} \right) = k \cdot t \tag{2}$$

where: Ct - concentration of organic compounds at time t during degradation [mg/dm³]; C_0 - concentration of organic compounds at time 0 during degradation [mg/dm³]; k - reaction rate constant [1/min]; t - time [min].

The degradation half-life, of investigated compounds was determined using equation:

$$t_{1/2} = \frac{\ln 2}{k} \tag{3}$$

Results and discussion

SEM and EDX analyses

In Figure 1a and b SEM picture and EDX analysis of PVA/GK (80/20, w/w) membrane, is shown respectively. The reason for chosen ratio between PVA and GK and

the exact characteristics of this membrane can be found in [31]. In Figure 1c and d SEM/EDX pictures of electrospun membrane with the addition of TiO_2 can be seen, whereas in e) and f) the same membrane but plasma treated is shown.
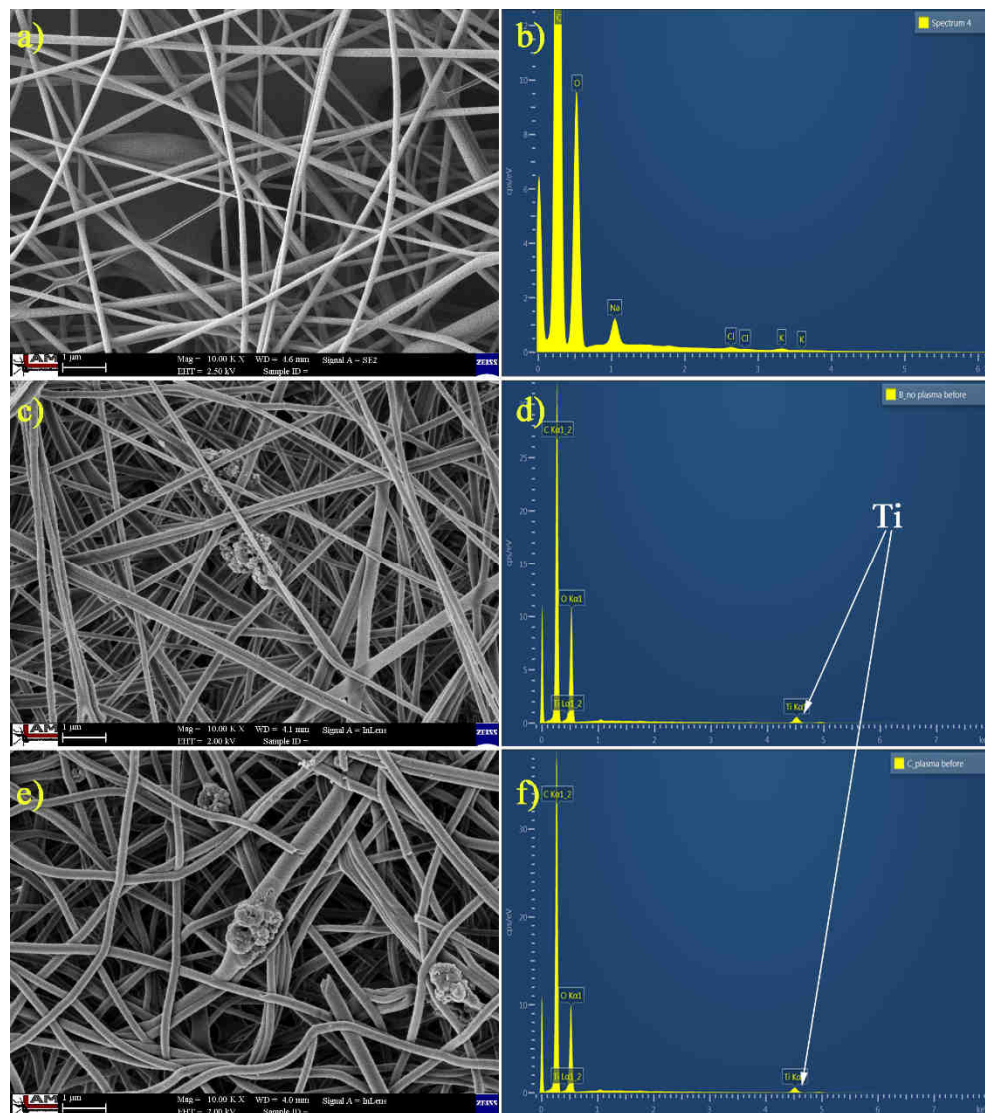

Fig. 1. SEM and EDX analysis of: a) and b) PVA/GK electrospun membrane, c) and d) PVA/GK electrospun TiO_2 membrane, and e) and f) PVA/GK plasma treated TiO_2 membrane

Fine nanoparticles of TiO_2 tightly attached to the fibers can be seen on both of the membranes.

Furthermore, the plasma treatment not only made the membrane more hydrophobic (as further shown in the section describing the water contact angle) but also more resistant to UV/Vis radiation which allowed to recover the membrane after the treatment of micro pollutants.
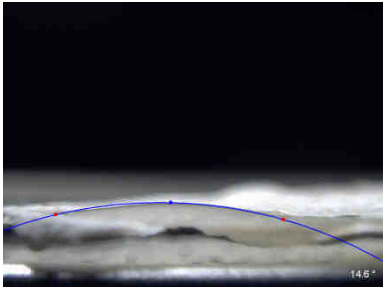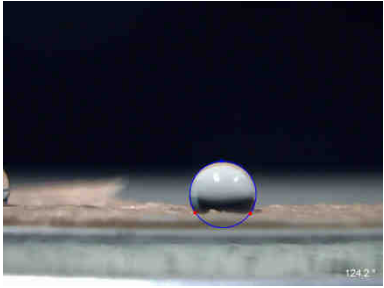
In addition, EDX analysis had revealed presence of TiO$_2$ component in both membranes (Figs. 1d and f). Furthermore, after the treatment polymerisation of the membrane occurred, although EDX analysis revealed that TiO$_2$ has remained on the membrane (data not shown).

Water contact angle measurements

Water contact angle measurements (WCA) were made for the membranes: PVA/GK electrospun TiO$_2$ membrane and PVA/GK plasma treated TiO$_2$ membrane (Table 2).

Table 2

Water contact angle measurements of PVA/GK electrospun TiO$_2$ membrane,
and PVA/GK plasma treated TiO$_2$ membrane

Sample name	Contact angle* [°]	Photo documentation
TiO$_2$ membrane	14.4±0.9	
Plasma treated TiO$_2$ membrane	121.2±9.4	

*measurements were replicated 3 times, error is presented as a standard deviation

WCA measurement is used to determine a surface hydrophilicity or hydrophobicity i.e. larger value of WCA indicates materials greater hydrophobicity. Many studies have already found that after methane plasma treatment, surface of the fiber is not only more hydrophobic but the grafted functional groups enhance its sorption capacity [31]. The surface of plasma treated TiO$_2$ membrane did not allow the water to spread evenly and created water droplet, therefore can be considered as very hydrophobic in nature, in contrary to the membrane without the methane plasma treatment.

Thermogravimetric analysis

Thermogravimetric analysis (TGA) was performed for the membranes without and with TiO_2 (and before/after plasma treatment).
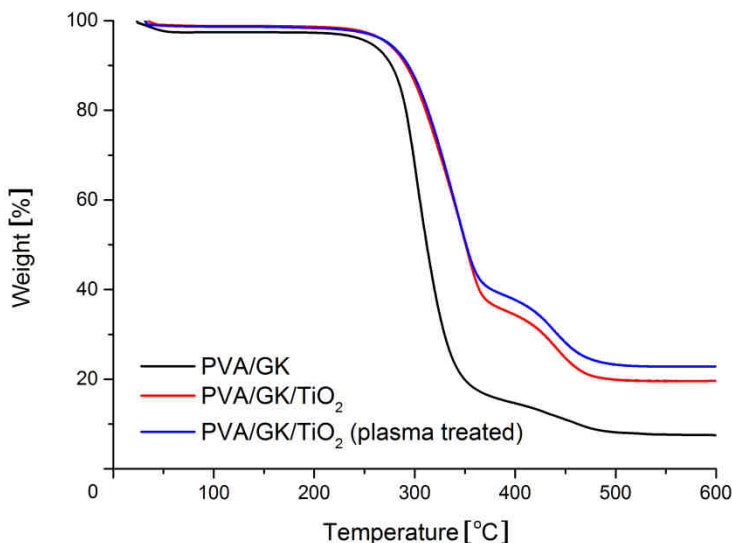

Fig. 2. TGA curves of PVA/GK electrospun membrane, PVA/GK electrospun TiO_2 membrane, and PVA/GK plasma treated TiO_2 membrane

From the TGA analysis, it is clear that all of the membranes degraded majorly in two steps up to a temperature of 600°C (Fig. 2). Thermogravimetric analysis estimated a TiO_2 content of approximately 12% for the PVA/GK/TiO_2 membrane.

Moreover, the thermal stability of the plasma treated membrane seems to be higher from the untreated one. These results also confirm that there was an insignificant loss of nanoparticles during the plasma treatment process.

ATR-FTIR spectroscopy

The ATR-FTIR spectra of PVA/GK electrospun membrane, PVA/GK electrospun TiO_2 membrane, and PVA/GK plasma treated TiO_2 membrane, are presented in Figure 3.

All of the membranes spectra shows peaks at 3300 cm^{-1} (related to the OH stretching vibration) and also at 1093 corresponding to –C-O-C– stretching vibrations of various sugar moieties present in the GK [31].

The bands around 2925 and 2850 cm^{-1} represents the characteristic vibration of C-H stretching while the peaks at 1418 and 1326 cm^{-1} are characteristic of the C-H deformation vibrations in PVA and GK. It was also observed that after the plasma treatment the bands around 2925 and 2850 cm^{-1} had lower intensity in comparison to the non-treated one due to probably destruction of a polymer chain structure.

Compared to PVA/GK membrane, new band with high intensity has been detected in the membrane with TiO_2 (1724 cm^{-1}) which is in agreement with the results obtained by Nasikhudin et al. [32]. Furthermore, the band at 1714 cm^{-1} has been ascribed to the

carbonyl group stretching modes probably of -COOH from gum karaya and ester groups from PVA copolymer. It has been reported that TiO$_2$ can absorb on polymers with -COOH group in two various schemes. One scheme is that TiO$_2$ can be bound with 2 oxygen atoms of COOH by a bidentate coordination to Ti^{4+} cation and the other one that it can form hydrogen bonding between carbonyl group and the surface hydroxyl group of TiO$_2$ [33].
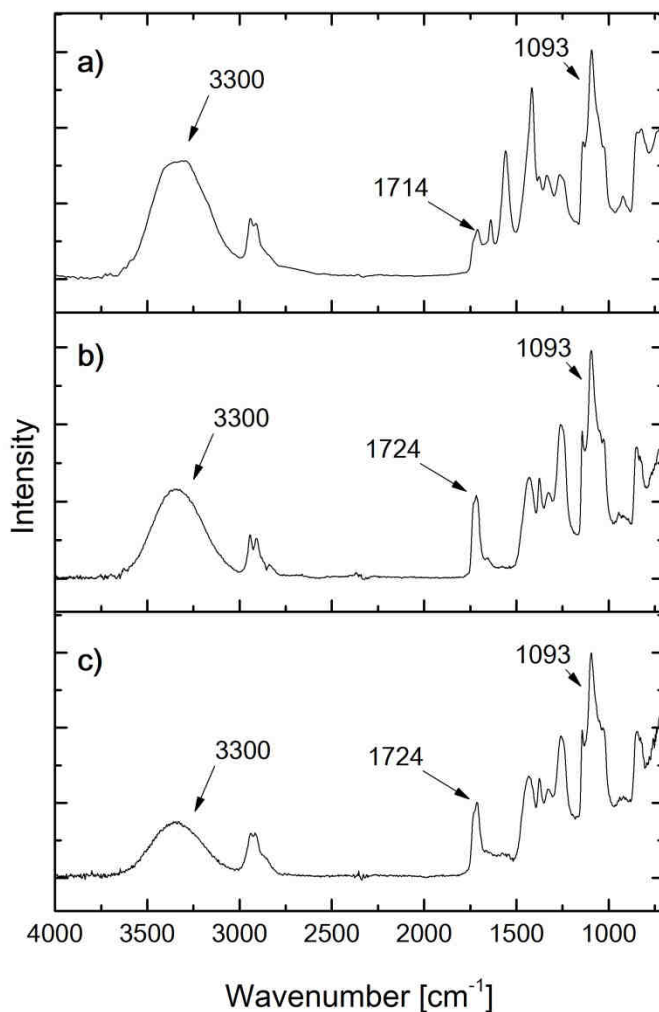

Fig. 3. FTIR analysis of: a) PVA/GK electrospun membrane, b) PVA/GK/TiO$_2$ membrane, and c) plasma treated PVA/GK/TiO$_2$ membrane

The additional functionality observed in the membrane after plasma treatment is due to the surface adjustment by grafting of hydroxyl, carbonyl, and carboxylate groups.

Membrane application for pharmaceutical removal

In Figure 4 there can be observed degradation process of BPA and DCF with UV and UV + TiO_2 deposited on electrospun membrane after plasma treatment. In the first stage of the study, the membrane containing TiO_2 was contacted for 15 min with the prepared water solutions. Due to the adsorption of micro pollutants on the catalyst and membrane surface, 18% reduction of BPA and 20% of DCF concentration was observed. These results indicate that the decomposition of both compound would take place mainly due to the reactions with reactive free radicals, such as $^•OH$, $O_2^{•-}$ and other oxygen species generated in the UV irradiated water solutions and not only during reactions on the catalyst surface.
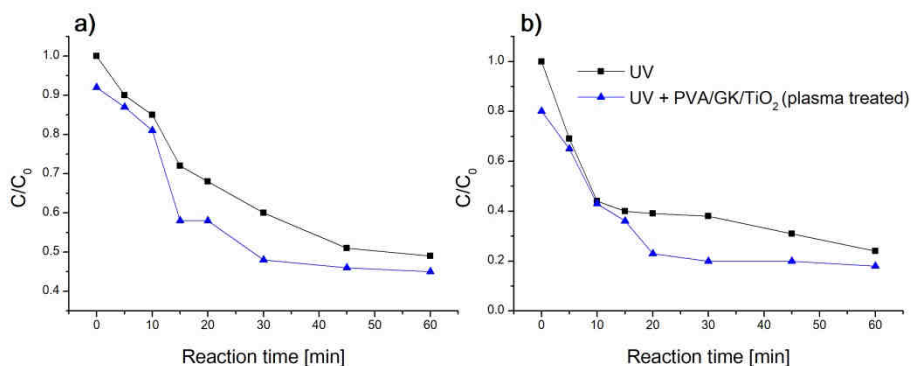

Fig. 4. Degradation of BPA (a) and DCF (b) during UV irradiation with and without TiO_2 membrane (temp. 20°C)

The inception of UV irradiation initiate the photochemical decomposition of organic compounds in the water solutions. The concentration of BPA decreased after 15 min by over 28%. The elongation of the process resulted in a removal degree of that micro pollutant which reached 60%. For DCF after only 10 min the removal degree of the drug exceeded 56% and increased to 76% after 60 min. The decomposition of the compound depends heavily on the process time and therefore on the dose of radiation supplied to the reaction mixture [34].

As expected the addition of the TiO_2 membrane, enhanced the decomposition process of both micro pollutants. Which is consistent with the results obtained by other researchers experimenting with TiO_2 nanoparticles [35]. The removal degree of BPA after 30 min in both processes reaches 50%. A higher efficiency was recorded for DCF whose concentration was reduced after 30 min of irradiation by more than 80%. Higher degrees of removal of the pharmaceutical compound in similar process conditions reaches 90% were observed by the use of TiO_2 as a mixture of anatase and rutile [36]. However, the presence of rutile does not positively affect the removal of BPA [37].

The calculated process kinetics (Table 3) indicate that the decomposition DCF and BPA was divided into two stages. A similar dependence was also observed during the photooxidation of other pharmaceutical compounds such as carbamazepine [38]. In the first 20 minutes of UV irradiation the half-life of BPA was about 27 minutes and with continued irradiation it reached for the UV + TiO_2 membrane process a value of 79.87 min^{-1}. Slower oxidation of the compound was also expressed by a decreasing value

of the reaction rate constant. This dependence was especially marked in the case of DCF removal. The reaction rate constant determined for the single UV process was in the first 10 min of irradiation more than four times higher. Also for processes supported by the presence of TiO$_2$ membrane the reaction rate constant significantly decreased after the first 20 min. The half-life of DCL for the UV + TiO$_2$ membrane process, in the second stage was extended about ten times. The inhibition of decomposition of micro pollutants can be caused by a competitive oxidation of decomposition by-products from the parent compounds.

Table 3

Decomposition half-lives of investigated micro pollutants obtained for the photolysis
(with and without membrane) process

Compound	Treatment process	Reaction time t [min]	Reaction rate constant k [min^{-1}]	R^2	Half-life $t_{1/2}$ [min]
BPA	UV	0-20	0.0122	0.93	63.15
	UV + Membrane	0-20	0.0266	0.88	27.52
		20-60	0.0161	0.81	79.87
DCF	UV	0-10	0.0821	0.99	8.28
		10-60	0.0197	0.92	74.69
	UV + Membrane	0-20	0.0617	0.98	14.17
		20-60	0.0147	0.89	148.55

Conclusions

In this study, nano-TiO$_2$ electrospun membrane was fabricated and used for the removal of two toxic organic compounds. The SEM/EDX morphology and elemental composition analysis revealed that the membrane has nano-TiO$_2$ particles attached, but it is not immune to the UV/Vis radiation and dissolves in the water rapidly. However, it was observed that plasma treated membrane could last longer and the dissolution of it does not happen as fast. The created herein membrane was then analysed with several analytical techniques, i.e. FTIR spectroscopy, TGA and water contact angle analyses. In addition, the membrane had shown higher efficiency towards degradation of bisphenol A and diclofenac in comparison to the bare UV process. Moreover, the calculated process kinetics indicated that the decomposition DCF and BPA can been divided into two stages. It is also believed that thus created membrane can help to recover TiO$_2$ after the treatment.

Acknowledgements

References

[1] Bhardwaj N, Kundu SC. Electrospinning: A fascinating fiber fabrication technique. Biotechnol Adv. 2010;28:325-47. DOI: 10.1016/j.biotechadv.2010.01.004.

[2]   Hwang S, Jeong S. Electrospun nano composites of poly(vinyl pyrrolidone)/nano-silver for antibacterial materials. J Nanosci Nanotechnol. 2011;11:610-613. DOI: 10.1166/jnn.2011.3243.

[3]   Deniz AE, Vural HA, Ortaç B, Uyar T. Gold nanoparticle/polymer nanofibrous composites by laser ablation and electrospinning. Mater Lett. 2011;65:2941-2943. DOI: 10.1016/j.matlet.2011.06.045.

[4]   Savva I, Krekos G, Taculescu A, Marinica O, Vekas L, Krasia-Christoforou T. Fabrication and characterization of magnetoresponsive electrospun nanocomposite membranes based on methacrylic random copolymers and magnetite nanoparticles. J Nanomater. 2012;2012:1-9. DOI: 10.1155/2012/578026.

[5]   Padil VVT, Filip J, Suresh KI, Wacławek S, Černík M. Electrospun membrane composed of poly[acrylonitrile-co-(methyl acrylate)-co-(itaconic acid)] terpolymer and ZVI nanoparticles and its application for the removal of arsenic from water. RSC Adv. 2016;6:110288-110300. DOI: 10.1039/C6RA24036D.

[6]   Gupta SM, Tripathi M. A review of TiO_2 nanoparticles. Chinese Sci Bull. 2011;56:1639-1657. DOI: 10.1007/s11434-011-4476-1.

[7]   Han H, Bai R. Buoyant photocatalyst with greatly enhanced visible-light activity prepared through a low temperature hydrothermal method. Ind Eng Chem Res. 2009;48:2891-2898. DOI: 10.1021/ie801362a.

[8]   Hamdi A, Ferreira DP, Ferraria AM, Conceição DS, Vieira Ferreira LF, Carapeto AP, et al. TiO_2-CdS nanocomposites: Effect of CdS oxidation on the photocatalytic activity. J Nanomater. 2016;2016:1-11. DOI: 10.1155/2016/6581691.

[9]   García-Mendoza C, Oros-Ruiz S, Hernández-Gordillo A, López R, Jácome-Acatitla G, Calderón HA, et al. Suitable preparation of Bi_2S_3 nanorods-TiO_2 heterojunction semiconductors with improved photocatalytic hydrogen production from water/methanol decomposition. J Chem Technol Biotechnol. 2016;91:2198-2204. DOI: 10.1002/jctb.4979.

[10] Baia L, Orbán E, Fodor S, Hampel B, Kedves EZ, Saszet K, et al. Preparation of TiO_2/WO_3 composite photocatalysts by the adjustment of the semiconductors' surface charge. Mater Sci Semicond Process. 2016;42:66-71. DOI: 10.1016/j.mssp.2015.08.042.

[11] Han H, Riboni F, Karlicky F, Kment S, Goswami A, Sudhagar P, et al. α-Fe_2O_3/TiO_2 3D hierarchical nanostructures for enhanced photoelectrochemical water splitting. Nanoscale. 2017;9:134-142. DOI: 10.1039/C6NR06908H.

[12] Singh N, Pandey V, Singh N, Malik MM, Haque FZ. Application of TiO_2/SnO_2 nanoparticles in photoluminescence based fast ammonia gas sensing. J Opt. 2017;46:199-203. DOI: 10.1007/s12596-017-0404-3.

[13] Li N, Li Y, Li W, Ji S, Jin P. One-step hydrothermal synthesis of TiO_2@MoO_3 core-shell nanomaterial: microstructure, growth mechanism, and improved photochromic property. J Phys Chem C. 2016;120:3341-3349. DOI: 10.1021/acs.jpcc.5b10752.

[14] Jampílek J, Král'ová K. Application of nanotechnology in agriculture and food industry, its prospects and risks. Ecol Chem Eng S. 2015;22:321-361. DOI: 10.1515/eces-2015-0018.

[15] Leong S, Razmjou A, Wang K, Hapgood K, Zhang X, Wang H. TiO_2 based photocatalytic membranes: A review. J Memb Sci. 2014;472:167-184. DOI: 10.1016/j.memsci.2014.08.016.

[16] Bet-moushoul E, Mansourpanah Y, Farhadi K, Tabatabaei M. TiO_2 nanocomposite based polymeric membranes: A review on performance improvement for various applications in chemical engineering processes. Chem Eng J. 2016;283:29-46. DOI: 10.1016/j.cej.2015.06.124.

[17] Michałowicz J. Bisphenol A - Sources, toxicity and biotransformation. Environ Toxicol Pharmacol. 2014;37:738-758. DOI: 10.1016/j.etap.2014.02.003.

[18] Chronopoulou L, Palocci C, Valentino F, Pettiti I, Wacławek S, Černík M, et al. Stabilization of iron (micro)particles with polyhydroxybutyrate for in situ remediation applications. Appl Sci. 2016;6:417. DOI: 10.3390/app6120417.

[19] Zhang L, Zeng Y, Cheng Z. Removal of heavy metal ions using chitosan and modified chitosan: A review. J Mol Liq. 2016;214:175-191. DOI: 10.1016/j.molliq.2015.12.013.

[20] Alsbaiee A, Smith BJ, Xiao L, Ling Y, Helbling DE, Dichtel WR. Rapid removal of organic micropollutants from water by a porous β-cyclodextrin polymer. Nature. 2015;529:190-194. DOI: 10.1038/nature16185.

[21] Singha AS, Guleria A. Use of low cost cellulosic biopolymer based adsorbent for the removal of toxic metal ions from the aqueous solution. Sep Sci Technol. 2014;49:2557-2567. DOI: 10.1080/01496395.2014.929146.

[22] Jeon C, Park JY, Yoo YJ. Novel immobilization of alginic acid for heavy metal removal. Biochem Eng J. 2002;11:159-166. DOI: 10.1016/S1369-703X(02)00020-7.

[23] Thakur S, Kumari S, Dogra P, Chauhan GS. A new guar gum-based adsorbent for the removal of Hg(II) from its aqueous solutions. Carbohydr Polym. 2014;106:276-282. DOI: 10.1016/j.carbpol.2014.02.041.

[24] Wacławek S, Chronopoulou L, Petrangeli Papini M, Vinod VTP, Palocci C, Kupčík J, et al. Enhancement of stability and reactivity of nanosized zero-valent iron with polyhydroxybutyrate. Desalin Water Treat. 2017;69. DOI: 10.5004/dwt.2017.0704.

[25] Padil VVT, Wacławek S, Senan C, Kupčík J, Pešková K, Černík M, et al. Gum karaya (Sterculia urens) stabilized zero-valent iron nanoparticles: Characterization and applications for the removal of chromium and volatile organic pollutants from water. RSC Adv. 2017;7:13997-14009. DOI: 10.1039/C7RA00464H.

[26] Wacławek S, Lutze HV, Grübel K, Padil VVT, Černík M, Dionysiou DD. Chemistry of persulfates in water and wastewater treatment: A review. Chem Eng J. 2017;330:44-62. DOI: 10.1016/j.cej.2017.07.132.

[27] Wacławek S, Antoš V, Hrabák P, Černík M. Remediation of hexachlorocyclohexanes by cobalt-mediated activation of peroxymonosulfate. Desalin Water Treat. 2016;57:26274-26279. DOI: 10.1080/19443994.2015.1119757.

[28] Yaqoob S, Ullah F, Mehmood S, Mahmood T, Ullah M, Khattak A, et al. Effect of waste water treated with TiO$_2$ nanoparticles on early seedling growth of Zea mays L. J Water Reuse Desalin. 2017. DOI: 10.2166/wrd.2017.163.

[29] Yang S, Hai FI, Nghiem LD, Nguyen LN, Roddick F, Price WE. Removal of bisphenol A and diclofenac by a novel fungal membrane bioreactor operated under non-sterile conditions. Int Biodeterior Biodegradation. 2013;85:483-490. DOI: 10.1016/j.ibiod.2013.03.012.

[30] Khuzwayo Z, Chirwa EMN. Analysis of catalyst photo-oxidation selectivity in the degradation of polyorganochlorinated pollutants in batch systems using UV and UV/TiO$_2$. South African J Chem Eng. 2017;23:17-25. DOI: 10.1016/j.sajce.2016.12.002.

[31] Padil VVT, Senan C, Wacławek S, Černík M. Electrospun fibers based on Arabic, karaya and kondagogu gums. Int J Biol Macromol. 2016;91:299-309. DOI: 10.1016/j.ijbiomac.2016.05.064.

[32] Nasikhudin, Ismaya EP, Diantoro M, Kusumaatmaja A, Triyana K. Preparation of PVA/TiO$_2$ Composites Nanofibers by using Electrospinning Method for Photocatalytic Degradation. IOP Conf. Ser. Mater. Sci. Eng. vol. 202, 2017. DOI: 10.1088/1757-899X/202/1/012011.

[33] Li J-H, Xu Y-Y, Zhu L-P, Wang J-H, Du C-H. Fabrication and characterization of a novel TiO$_2$ nanoparticle self-assembly membrane with improved fouling resistance. J Memb Sci. 2009;326:659-666. DOI: 10.1016/j.memsci.2008.10.049.

[34] Kovacic M, Juretic Perisic D, Biosic M, Kusic H, Babic S, Loncaric Bozic A. UV photolysis of diclofenac in water; kinetics, degradation pathway and environmental aspects. Environ Sci Pollut Res. 2016;23:14908-14917. DOI: 10.1007/s11356-016-6580-x.

[35] Bodzek M, Rajca M. Photocatalysis in the treatment and disinfection of water. Part I. Theoretical backgrounds. Ecol Chem Eng S. 2012;19:489-512. DOI: 10.2478/v10216-011-0036-5.

[36] Bohdziewicz J, Kudlek E, Dudziak M. Influence of the catalyst type (TiO$_2$ and ZnO) on the photocatalytic oxidation of pharmaceuticals in the aquatic environment. Desalin Water Treat. 2016;57:1552-1563. DOI: 10.1080/19443994.2014.988411.

[37] Wang R, Ren D, Xia S, Zhang Y, Zhao J. Photocatalytic degradation of Bisphenol A (BPA) using immobilized TiO$_2$ and UV illumination in a horizontal circulating bed photocatalytic reactor (HCBPR). J Hazard Mater. 2009;169:926-932. DOI: 10.1016/j.jhazmat.2009.04.036.

[38] Chong MN, Jin B. Photocatalytic treatment of high concentration carbamazepine in synthetic hospital wastewater. J Hazard Mater. 2012;199-200:135-142. DOI: 10.1016/j.jhazmat.2011.10.067.